Structures 44 (2022) 1138–1151

Contents lists available at ScienceDirect

Structures

journal homepage: www.elsevier.com/locate/structures

Effect of opening shape, size and location on the punching shear behaviour of RC flat slabs

Tarek F. El-Shafiey [a], Ahmed M. Atta [a], Ali Hassan [b,*], Mohamed Elnasharty [c]

[a] Concrete Structures, Department of Structural Engineering, Faculty of Engineering, Tanta University, Tanta, Egypt
[b] Department of Structural Engineering, Faculty of Engineering, Tanta University, Tanta, Egypt
[c] Structural Engineering Dept., Faculty of Engineering, Tanta University, Tanta, Egypt

ARTICLE INFO

Keywords:
Two-way RC slabs
Opening
Punching shear
Concrete
Slab-column connection

ABSTRACT

The current study aims to investigate the effect of opening size, location and shape on the punching shear behaviour of Reinforced Concrete (RC) flat slabs. Ten two-way slabs with a span of 1600 mm and a thickness of 120 mm were tested under a static load applied on a central stub column. The test program was divided into three groups with openings and a control slab without opening. Group I was designed to study the effect of opening size, thus, three slabs with three different opening sizes were tested. The openings dimensions were 200 × 200, 300 × 300 and 400 × 400 mm^2. These openings were created beside the column. On the other hand, in group II, three slabs with the same opening size of 300 × 300 mm^2 were tested, when the openings were at different locations. The distances between the opening edge and the column face were 100, 200 and 300 mm. To study the effect of opening shape, the slabs of group III having circular openings were tested. The openings' diameters were 250, 350 and 450 mm, these values were configured to equalize the areas of the square openings of group I. The test results indicated that the slabs' capacities and stiffness notably decreased with increasing the opening size. However, the percentage of the decrease could be reduced by increasing the distance between the column and the opening and/or using a circular opening. The ultimate experimental punching shear capacities of slabs with openings were compared with those obtained by the equations of ECP-203, *ACI*-318 and EC2 codes. Based on this comparison, ECP-203 and *ACI*-318 showed higher factors of safety than EC2.

1. Introduction

A common floor system is the two-way Reinforced Concrete (RC) flat slab supported by columns. The absence of projected beams in flat slabs increases the clear height of the floor as well as reduces the construction time and labor [1]. Nevertheless, at the slab-column connection, complex behaviour is developed owing to the superposition of flexural and shear stresses beside the column. In addition, one of the main problems with the flat slab floor systems is their capability to the premature punching shear failure. The punching shear failures occur without any warning signs, furthermore, the punching shear cracks occur in the top fibers of the slab, which are usually not visible due to the existence of a flooring cover [2–8]. Thus, the punching shear must be carefully checked at the design stage. Openings in RC flat slabs may be required for many architectural reasons, such as; providing elevators or stairways to provide connections among floors or providing gas, water, electricity, and air conditioning systems. In many cases, openings may be positioned very close to the columns, which highly affects the punching shear behaviour of the flat slabs.

Many research work was done to study the punching shear behaviour of flat slabs with openings. Table 1, presents a summary of the available test parameters and main results of previous investigations. EL-Shafiey et al. [9] studied the effect of openings size and location on the punching shear behaviour of RC flat slabs. As per El-Shafiey et al. findings, the punching shear capacities of tested specimens with openings significantly reduced. The percentage of these reductions ranged between 20.61 and 50.82% of that carried by the control slab. Also, Anil et al. [10] studied the effect of opening size and location on the punching shear behaviour of RC flat slabs. The tests were carried out on eight two-way RC flat slabs having openings with variable positions. Each test slab has one opening with the dimensions of 300 × 300 mm or 500 × 500 mm located next to the column or 300 mm far from the central column in a parallel or a diagonal position. As per Anil et al. recommendations, the punching shear capacity decreases with increasing the opening size, moreover, the percentage of the decrease for openings adjacent to the

* Corresponding author at: Faculty of Engineering, Tanta University, Tanta 31511, Egypt.
E-mail address: Ali_hassan@f-eng.tanta.edu.eg (A. Hassan).

https://doi.org/10.1016/j.istruc.2022.08.076
Received 25 May 2022; Received in revised form 2 August 2022; Accepted 16 August 2022
Available online 23 August 2022
2352-0124/© 2022 Institution of Structural Engineers. Published by Elsevier Ltd. All rights reserved.

Nomenclatures

a	shorter side of column
b	longer side of column
b_o	shear perimeter, mm units
$C_{Rd,c}$	experimental factor, $C_{Rd,c} = 0.18$
d	effective slab's depth, mm units
f_{ck}, $f_c^{'}$	cylindrical compressive strength for concrete, MPa units
f_{cu}	cubic compressive strength for concrete, MPa units
k	coefficient of effective height
V_c	shear force carried by concrete
α, α_s	coefficient of column location, $\alpha = \alpha = 4$ for interior column
β	ratio of longer side to shorter side of column
λ	loading coefficient, $\lambda = 1.0$ in the case of axial load
ρ	longitudinal reinforcement ratio
ρ_{cp}	compressive reinforcement ratio

results indicated that the ultimate capacity, stiffness and energy dissipation of the flat slabs with openings significantly decreased compared to the reference solid slab. Elsayed et al. [13] studied the effect of crumb rubber on the punching shear capacity of flat slabs with openings. It was concluded that providing an opening adjacent to the column face caused a significant reduction in the punching shear capacity, and the capacity decreased with the increase in opening size [13]. The average ratios of reductions were about 24 and 35% for the slabs with openings of 100x100 and 150x150 mm, respectively. Genikomsou and Polak [14] carried out a finite element model to evaluate the effect of openings in RC slabs without shear reinforcement. The numerical results confirmed that the punching shear resistance decreased with increasing the opening size [14]. Also, Mostofinejad et al. [15] used a finite element model to investigate the effects of openings varying in location and size on the punching shear strength of flat slabs. The results demonstrated that providing openings beside columns caused a remarkable increase in the shear stress around the slab-column connections. Moreover, a significant increase in the stresses around the openings was observed [15]. Teng et al. [16] studied the punching shear behaviour of two-way RC slabs with openings supported on rectangular columns. Teng et al. concluded

Table 1a
Summary of test parameters for previous work [9–11].

Ref.	Specimen	Specimen dimensions, mm^3	Column dimensions, mm^2	f_c, MPa	μ, %	Opening size, mm^2	Opening location to column	P_u, kN	R, %
EL-Shafiey et al. [9]	1	1700 × 1700 × 120	200 × 200	24.00	0.9	–	–	427	–
	2	1700 × 1700 × 120	200 × 200	24.00	0.9	200 × 200	Adjacent, parallel	315	26.23
	3	1700 × 1700 × 120	200 × 200	24.00	0.9	300 × 300	Adjacent, parallel	222	48.01
	4	1700 × 1700 × 120	200 × 200	24.00	0.9	400 × 400	Adjacent, parallel	210	50.82
	5	1700 × 1700 × 120	200 × 200	24.00	0.9	200 × 200	Adjacent, diagonal	339	20.61
	6	1700 × 1700 × 120	200 × 200	24.00	0.9	300 × 300	Adjacent, diagonal	300	29.74
	7	1700 × 1700 × 120	200 × 200	24.00	0.9	400 × 400	Adjacent, diagonal	261	38.87
Anil et al. [10]	1	2000 × 2000 × 120	200 × 200	20.83	0.39	–	–	193	–
	2	2000 × 2000 × 120	200 × 200	20.60	0.39	300 × 300	Adjacent, parallel	99.03	48.60
	3	2000 × 2000 × 120	200 × 200	20.85	0.39	300 × 300	Adjacent, diagonal	125.86	34.78
	4	2000 × 2000 × 120	200 × 200	19.63	0.39	500 × 500	Adjacent, parallel	76.98	60.11
	5	2000 × 2000 × 120	200 × 200	19.61	0.39	500 × 500	Adjacent, diagonal	94.70	50.93
	6	2000 × 2000 × 120	200 × 200	20.02	0.39	300 × 300	Parallel, 300 mm far	134.78	30.16
	7	2000 × 2000 × 120	200 × 200	21.24	0.39	300 × 300	Diagonal, 300 mm far	172.15	10.80
	8	2000 × 2000 × 120	200 × 200	20.05	0.39	500 × 500	Parallel, 300 mm far	115.53	40.13
	9	2000 × 2000 × 120	200 × 200	20.23	0.39	500 × 500	Diagonal, 300 mm far	138.83	28.06
Elsayed et al. [11]	1	1000 × 1000 × 65	100 × 100	32.4	0.82	–	–	97.5	–
	2	1000 × 1000 × 65	100 × 100	32.4	0.82	100 × 100	Adjacent, parallel	69.5	28.72
	3	1000 × 1000 × 65	100 × 100	32.4	0.82	100 × 100	Adjacent, diagonal	88.5	9.232
	4	1000 × 1000 × 65	100 × 100	32.4	0.82	100 × 100	Parallel, 25 mm far	74.5	23.59
	5	1000 × 1000 × 65	100 × 100	32.4	0.82	100 × 100	Parallel, 50 mm far	81.3	16.62
	6	1000 × 1000 × 65	100 × 100	32.4	0.82	100 × 100	Parallel, 75 mm far	83.3	14.56
	7	1000 × 1000 × 65	100 × 100	32.4	0.82	100 × 100	Parallel, 100 mm far	88.5	9.23

f_c = cylinder compressive strength; μ = tensile reinforcement ratio; P_u = ultimate load; R = reduction in ultimate load due to opening.

column is higher than that for openings located away from the column. The maximum reduction in the ultimate capacity was obtained by a slab having an opening of 500 × 500 mm. The ultimate capacity was about 40% of that of the control slab. Elsayed et al. [11] studied the punching shear behaviour of two-way RC flat slabs with openings supported by square interior coupled columns. Three variables were considered in this research, which were the separation distance of the columns (d, 2d, 3d, and 4d), the location of the opening, and the distance from column face to the opening. Elsayed et al. concluded that the punching shear capacity increased by increasing the clear distance between columns. The decrease in punching shear capacity of slabs with openings ranged between 10 and 32% compared to the control specimen without opening. Liberati et al. [12] studied the shear failure of flat slabs with openings adjacent to columns. Twelve RC flat slabs with dimensions of 1800 × 1800 × 130 mm^3 without any shear reinforcement were tested. The test

that the openings considerably reduced the punching strength of the tested slabs and the best location for the opening was along the longer side of the column.

Based on the literature review, the previous studies of two-way RC slabs with openings focused on the effect of openings size/location on the punching shear behaviour of RC slabs. On the other hand, comprehensive research on the punching shear behaviour of RC slabs considering variations in the shape/size of openings has not been found. Thus, the current study was carried out to assess the effect of varying parameters on the punching shear response of two-way RC slabs. The studied parameters were the opening size, shape and location. The effects of these parameters were interpreted by examining the ultimate loads, cracking pattern, cracking load and load–deflection of ten test slabs. Finally, in the last part of this study, the experimental punching shear capacities of the tested slabs were compared with the predicted by

Table 1b
Summary of test parameters for previous work [12,13].

s	Specimen	Specimen dimensions, mm^3	Column dimensions, mm^2	f_c, MPa	μ, %	Opening size, mm^2	Opening location to column	P_u, kN	R, %
Liberati et al. [12]	1	1800 × 1800 × 130	150 × 150	41.6	1.62	–	–	249.9	–
	2	1800 × 1800 × 130	150 × 150	41.6	1.65	–	–	216.4	–
	3	1800 × 1800 × 130	150 × 150	41.6	1.58	–	–	259.2	–
	4	1800 × 1800 × 130	150 × 150	39.8	1.58	–	–	232.3	–
	5	1800 × 1800 × 130	150 × 150	44.5	1.28	1 φ 50 mm	Adjacent to column	187.6	24.93
	6	1800 × 1800 × 130	150 × 150	44.5	1.34	1 φ 50 mm	Adjacent to column	178.0	33.22
	7	1800 × 1800 × 130	150 × 150	44.5	1.26	1 φ 50 mm	Adjacent to column	233.7	9.83
	8	1800 × 1800 × 130	150 × 150	35.2	1.14	2 φ 150 mm	Adjacent to column	187.6	24.93
	9	1800 × 1800 × 130	150 × 150	35.2	1.08	2 φ 150 mm	Adjacent to column	213.9	1.11
	10	1800 × 1800 × 130	150 × 150	35.2	1.12	2 φ 150 mm	Adjacent to column	194.8	24.84
	11	1800 × 1800 × 130	150 × 150	41	1.17	2 φ 150 mm	Adjacent to column	208.4	10.28
	12	1800 × 1800 × 130	150 × 150	40	1.29	4 φ 75 mm	Adjacent to column	184.0	26.37
Elsayed M et al. [13]	1	1000 × 1000 × 100	100 × 100	31.6	0.66	–	–	182.9	–
	2	1000 × 1000 × 100	100 × 100	30.3	0.66	–	–	176.7	
	3	1000 × 1000 × 100	100 × 100	27.7	0.66	–	–	154.9	
	4	1000 × 1000 × 100	100 × 100	46.6	0.66	–	–	150.0	
	5	1000 × 1000 × 100	100 × 100	31.6	0.66	100 × 100	Adjacent to column	140.2	23.34
	6	1000 × 1000 × 100	100 × 100	30.3	0.66	100 × 100	Adjacent to column	137.0	22.46
	7	1000 × 1000 × 100	100 × 100	27.7	0.66	100 × 100	Adjacent to column	119.2	23.04
	8	1000 × 1000 × 100	100 × 100	46.6	0.66	100 × 100	Adjacent to column	109.2	27.20
	9	1000 × 1000 × 100	100 × 100	31.6	0.66	150 × 150	Adjacent to column	120.4	34.17
	10	1000 × 1000 × 100	100 × 100	30.3	0.66	150 × 150	Adjacent to column	118.2	33.11
	11	1000 × 1000 × 100	100 × 100	27.7	0.66	150 × 150	Adjacent to column	100.9	34.86
	12	1000 × 1000 × 100	100 × 100	46.6	0.66	150 × 150	Adjacent to column	91.6	38.93

f_c = cylinder compressive strength; μ = tensile reinforcement ratio; P_u = ultimate load; R = reduction in ultimate load due to opening.

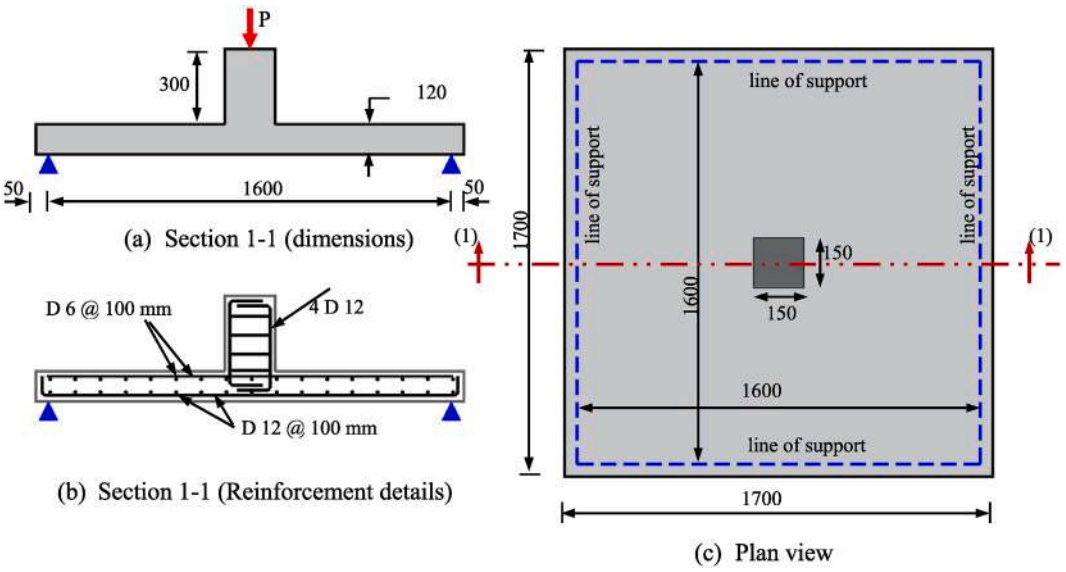


Fig. 1. Details of the control slab (All dimensions in mm).

the available codes.

2. Experimental work program

2.1. Test specimens

In this study, the experimental program consisted of ten two-way RC slabs. Figs. 1 and 2 shows the dimensions of the tested slabs. As shown in Fig. 1, the slabs have 1700 mm side length and 120 mm thickness. The specimens were manufactured with a central stub column. The stub column had a square cross-section with 150 mm side length and 300 mm height. All slabs were reinforced with constant top and bottom steel reinforcing meshes. For the bottom reinforcing mesh (tension reinforcement), D 12 mm steel bars with 100 mm spacing were used in both directions ($\mu_t = 1.13\%$). For the top reinforcing mesh, D 6 mm steel bars with 100 mm spacing were used in both directions ($\mu_c = 0.28\%$). It is worth mentioning that when the openings were created, the cut reinforcing bars due to the opening were compensated with similar continuous bars, which were provided at both sides of the opening. As shown in Fig. 1, the stub columns were reinforced with 4 vertical reinforcing bars of 12 mm diameter and D 6 mm with 75 mm spacing transversal stirrups.

Table 2 presents the test matrix of the current study. Fig. 2 shows the layout of the tested slabs with openings. As shown in Table 2, the test program contained a control specimen SC without an opening, in addition to, nine slabs with openings that were divided into three groups (three slabs per each). Group I was designed to study the effect of opening size on the punching shear behaviour. Thus, three different

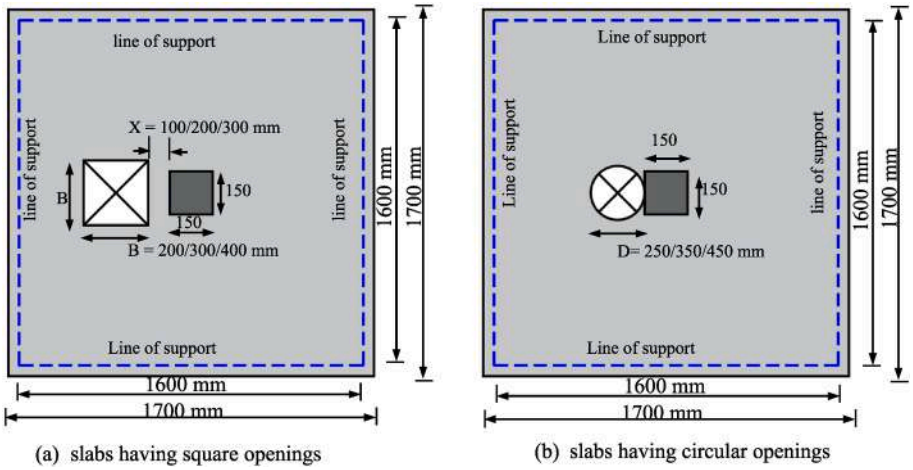


Fig. 2. Layout of the slabs having openings.

Table 2
Test parameters.

Group	Slab's designation	Opening shape	B or D, mm	X, mm	Objectives
Control	SC	–	–	–	Reference
Group I	S-SO-200-0	Square	200	0	Studying the effect of the opening's size
	S-SO-300-0	Square	300	0	
	S-SO-400-0	Square	400	0	
Group II	S-SO-300-100	Square	300	100	Studying the effect of the opening's location
	S-SO-300-200	Square	300	200	
	S-SO-300-300	Square	300	300	
Group III	S-CO-250-0	Circular	250	0	Studying the effect of the opening's shape
	S-CO-350-0	Circular	350	0	
	S-CO-450-0	Circular	450	0	

B or *D* = opening's length or diameter; *X* = distance from column face to the opening edge.

opening sizes were studied: 200 × 200, 300 × 300, and 400 × 400 mm^2. These openings were placed beside the stub column. Whereas, the slabs of group II were designed to study the effect of the opening location on the punching shear behaviour of RC slabs. Accordingly, three slabs with the same opening size of 300 × 300 mm^2 were tested, when the openings were at different locations. The distances between the opening edge and the column face were 100, 200 and 300 mm, these values represent one, two and three times the slab's effective depth (*d*), respectively. To study the effect of opening shape on the punching shear behaviour, the slabs of group III having circular openings were tested. The studied diameters were 250, 350 and 450 mm; these values were configured to equalize the areas of the square openings of group I.

2.2. Specimens' designation

As shown in Table 2, the control slab (without opening) was symbolized by the capital letters SC. On the other hand, the slabs with openings were designated by four symbols separated by dashes. The first symbol "S" refers to a slab with an opening. The second symbol refers to the shape of the opening (SO = Square Opening and CO = Circular Opening). The third symbol refers to the side length of the square opening or the diameter of the circular opening. Finally, the last symbol stands for the distance between the opening and the column face. For instance, the designation 'S-SO-200-200' refers to a slab with a square opening with a side length of 200 mm and this opening locates at 200 mm far from the column face.

Table 3
Characteristics of the used steel reinforcement.

Diameter, mm	Steel type[a]	Yield strength, MPa	Ultimate strength, MPa	Modulus of elasticity, GPa
6	B240D-P	245	362	205
12	B420DWR	422	615	205

[a] As per ECP-203 national code[17].

2.3. Material properties

In this study, all slabs were cast using a ready concrete mixture. The used mixture was designed to obtain an average cylindrical compressive strength of 24 MPa at 28 days. For one cubic meter, the weights of sand, crushed stone, water and cement were 387.5, 1175, 135 and 400 kg, respectively. The actual compressive strength at the test date was determined by the uniaxial compressive test of six standard cylinders (150 × 300 mm), which were preserved in the same conditions as the test slabs. At the test date, the average compressive strength of the tested cylinders was 24.02 MPa. On the other hand, the tensile strength of the used concrete was determined based on the splitting tensile test of three cylinders (150 × 300 mm). The average tensile strength of the used concrete was 3.05 MPa.

In the current experimental program, two grades of steel reinforcement were used: type B420DWR (yield strength = 420 MPa) for bars of 12 mm diameter and type B240D-P (yield strength = 220 MPa) for bars of 6 mm diameter. For the used steel reinforcement, the actual mechanical properties were determined using the uniaxial tensile test, which was carried out on three standard specimens for each diameter. Table 3 summarizes the average yield strength (f_{ty}), ultimate strength (f_{tu}), and the young's modulus (E) for the used steel reinforcement. As shown in Table 3, for the steel bars with a diameter of 6 mm, the f_{ty}, f_{tu}, and E were 245 MPa, 362 MPa and 205 GPa, respectively. For the bars with a diameter of 12 mm, the f_{ty}, f_{tu}, and E were 422 MPa, 615 MPa, and 205GPa, respectively.

2.4. Test setup and instrumentation

The used test setup and instrumentation details are shown in Fig. 3. As shown in Fig. 3, the tested slabs were placed over four simple supports along the four edges of the slabs. An incremental monotonic load was applied through a stub column using a load-controlled scheme with an average loading rate of about 10 kN/min till failure where the acting load was measured using a load cell of 400 kN capacity. As shown in Fig. 3, the vertical deflections were measured by using a set of LVDTs (linear variable displacement transducers) with an accuracy of 0.01 mm.

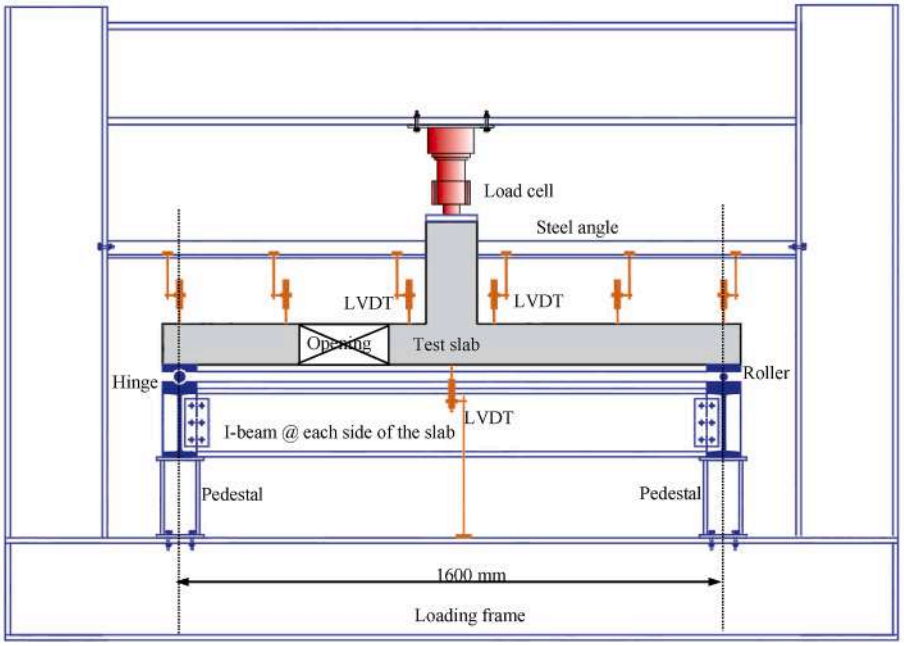


Fig. 3. Sketch of the test setup and instrumentation.

Electrical strain gauges (10 mm gauge length) were bonded to the middle of the continuous tension reinforcing bars to obtain the axial steel strains. The electrical resistance of the used strain gauges was 120 Ohms. The strain gauges, the LVDTs and the load cell were connected to an automatic data acquisition system.

3. Results and discussion

3.1. Cracking pattern and mode of failure

The failure modes of the slab-column connections of the tested slabs are shown in Fig. 4. In addition, sketches for the failure crack patterns of tested slabs are presented in Fig. 5, the proposed punching shear perimeters of ECP-203 [17], *ACI*-318 [18] and EC2 [19] codes were included in the figure for comparison. As per ECP-203 and *ACI*-318, the critical punching perimeter locates at 0.5d from the column face. Whereas, the critical punching perimeter locates at 2d from the column face according to EC2. For the control slab, the first radial crack was noticed at the slab's bottom face when the load reached about 65 kN. As the applied load increased, additional cracks propagated radially from the column's faces toward the edges of the slab. Reaching a load of 108 kN, the first circumferential crack formed around the column face. Increasing the applied load, other circumferential cracks formed parallel to the column perimeter. Finally, a sudden failure took place when the applied load reached about 235 kN. The failure was accompanied by a roaring sound and a complete penetration of the column to the top surface of the slab, indicating the occurrence of shear failure. As shown in Fig. 5, the failure-truncated cone is located at about 300 mm from the column face; this value represents three times the slab's effective depth. In addition, the formed cone has almost a circular shape with an average diameter of 735 mm. Comparing the obtained punching cone with those recommended by the design codes, EC2 showed the best prediction for the punching shear perimeter, whereas, *ACI* and ECP were very conservative.

For the slabs of group I, the radial cracks formed at the initial stages of loading, the first one took place at the corners of the opening near the column face and then extended toward the outer edges of the slab. At higher degrees of load, circumferential cracks appeared, forming the surface of the punching. Referring to the failure-cracking pattern of group I, the increase in opening width interrupted the transfer of loads in the x-direction, being the most of the loads transferred in the y-direction, this decreased the number of cracks formed in the left side of the slab including the opening. In addition, the diameter of the truncated concrete cone in the y-direction was larger than that in the x-direction. For slabs S-SO-200-0, S-SO-300-0 and S-SO-400-0, the diameters of the truncated cones in the y-direction were 750, 850 and 1000 mm, respectively, vs 700, 800 and 900 mm in the x-direction. Comparing the experimental punching perimeters of group I with the design codes, increasing the opening width increased the difference between the codes' perimeters and the experimental perimeters.

The slabs of group II exhibited similar cracking patterns similar to group I. The radial cracks started from the opening corner near the column, afterward, the circumferential took place. As can be seen in Fig. 5, as the distance (x) between the column and opening increased, the diameter of the truncated cone decreased and the shape of the cone became more regular. For slabs S-SO-300-100, S-SO-300-200 and S-SO-300-300, the average diameters of the truncated cones were 825, 750 and 735 mm, respectively. Also, while the distance × increases the punching perimeter of EC2 becomes closer to the experimental one, where, *ACI* and ECP-203 codes are still very conservative.

As for the slabs of group III, the radial cracks started from the column corner near the opening and then propagated toward the slab's edges, afterward, the circumferential took place. Comparing the cracks of groups II and III it is noticed that, while the radial cracks were intensive at the corners of the square opening, the cracks were distributed over the circumference of the circular opening. In addition, as the opening diameter increased, the average diameter of the punching cone was almost constant. For slabs S-CO-250-0, S-CO-350-0 and S-CO-450-0, the average diameters of the punching cones were 775, 790 and 725 mm, respectively. Also, all codes showed conservative predictions for the punching perimeter, however, EC2 was the closest one to that of the experimental test.

3.2. First crack loads

During the test, the slabs were visually observed until the occurrence of the first crack with the recording of the corresponding first crack load and deflection. Table 4 summarizes the first cracking loads for both



Fig. 4. Shear failure at the slab-column connection of the tested slabs.

radial (P_R) and tangential (P_{Tan1}) cracks. As presented in Table 4, the control slab recorded the height cracking capacity for both radial and tangential cracks. The values of P_R and P_{Tan1} for the control slab were 65 and 108 kN, respectively. On the other hand, it is evident that providing an opening beside the column dramatically decreased the first cracking loads. In addition, the reduction in first crack capacity increased with increasing the opening width. For slabs S-SO-200-0, S-SO-300-0 and S-SO-400-0, the values P_R were 85, 77 and 62%, respectively, of that achieved by the control slab and the values of P_{Tan1} were 0.75, 67 and 58%, respectively, of that achieved by the control slab.

The slabs of group II (having openings far from the column face) exhibited slight improvement in the first crack capacity in comparison with the slabs of group I (having openings next to the column face). Moreover, the effect of the opening reduced with increasing the distance between the opening and the column. For slabs S-SO-300-100, S-SO-300-200 and S-SO-300-300, the values P_R were 4, 10 and 20%, respectively, higher than that achieved by slab S-SO-300-0 and the values of P_{Tan1} were 5, 11 and 21%, respectively, higher than that achieved by slab S-SO-300-00-0.

Using a circular opening instead of a rectangular opening led to higher cracking loads with the slabs of group III when compared with their alternatives of group I. In addition, as shown in Table 4, the degree of enhancement in the first crack loads increased with increasing the opening size. For instance, slab S-CO-250-0 achieved cracking loads, P_R and P_{Tan1}, of 9 and 5%, respectively, higher than its counterpart slab (S-SO-200-0). On the other hand, slab S-CO-450-0 achieved cracking loads, P_R and P_{Tan1}, of 30 and 21%, respectively, higher than its counterpart slab (S-SO-400-0). The improvement in the cracking loads of the slabs with circular openings may be attributed to the absence of sharp edges, which increase the stress concentration around the opening corners.

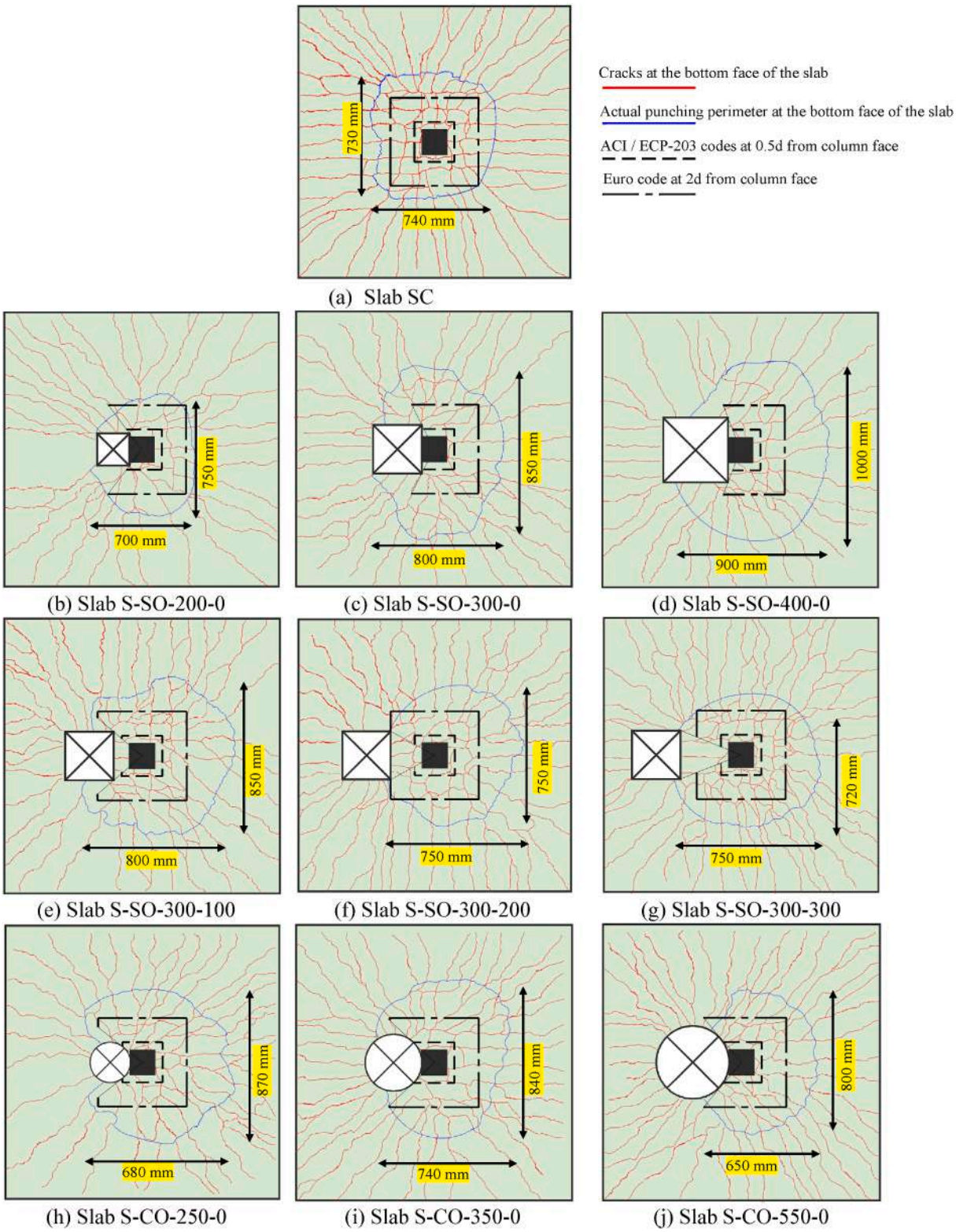


Fig. 5. Sketches of the final crack pattern of the tested slabs.

3.3. Ultimate loads

Table 5 presents the ultimate loads of the tested slabs. As expected, the control slab has the highest ultimate load capacity compared to the rest of the tested slabs. The control slab failed when the load reached about 235 kN. Fig. 6 presents a relation between the ultimate load/ultimate load of the control slab ($P_u/P_{u,sc}$) and, the opening width/slab depth (B/d). It was found that introducing an opening beside the column significantly reduced the punching shear capacity of the tested slabs. In addition, as the opening width increased, the reduction in the ultimate capacity increased. For slabs S-SO-200-0, S-SO-300-0 and S-SO-400-0, the ultimate loads were about 74, 61 and 49%, respectively, of that achieved by the control slab. This reduction is attributed to the loss of the effective critical section perimeter, which is important for the

Table 4
Cracking loads.

Group	Slab's designation	First radial crack load		First tangential crack load		Second tangential crack load		Third tangential crack load	
		P_R	WRT SC	P_{Tan1}	WRT SC	P_{Tan2}	WRT SC	P_{Tan3}	WRT SC
Control	SC	65	1.0	108	1.0	165	1.0	190	1.0
Group I	S-SO-200-0	55	0.85	90	0.75	132	0.80	158	0.83
	S-SO-300-0	50	0.77	80	0.67	122	0.74	143	0.75
	S-SO-400-0	40	0.62	70	0.58	102	0.62	123	0.65
Group II	S-SO-300-100	52	0.80	84	0.77	127	0.77	152	0.80
	S-SO-300-200	55	0.85	89	0.82	132	0.80	156	0.82
	S-SO-300-300	60	0.92	97	0.89	140	0.85	163	0.86
Group III	S-CO-250-0	60	0.92	95	0.83	141	0.85	160	0.84
	S-CO-350-0	55	0.85	90	0.79	132	0.80	150	0.79
	S-CO-450-0	52	0.80	85	0.75	124	0.75	143	0.75

P_R = load at first radial crack; P_{Tan1} = load at the first tangential crack; P_{Tan2} = load at the second tangential crack; P_{Tan3} = load at the third tangential crack; WRT SC = with respect to control slab SC.

Table 5
Summary of test results.

Group	Slab's designation	$P_{cr,Tan}$, kN	P_u, kN	$P_u/P_{u,SC}$	$P_u/P_{cr,Tan}$	Δ_u, mm	K, kN/mm
Control	SC	108	235	1.0	2.17	13.81	35.08
Group I	S-SO-200-0	90	175	0.74	1.94	10.84	27.84
	S-SO-300-0	80	143	0.61	1.79	10.54	24.01
	S-SO-400-0	70	115	0.49	1.64	8.82	20.26
Group II	S-SO-300-100	82	160	0.68	1.95	11.02	28.78
	S-SO-300-200	85	176	0.75	2.07	11.29	30.82
	S-SO-300-300	90	195	0.83	2.16	12.01	32.31
Group III	S-CO-250-0	95	180	0.77	1.89	11.76	32.15
	S-CO-350-0	90	170	0.72	1.89	11.65	26.50
	S-CO-450-0	85	150	0.64	1.76	11.40	22.52

$P_{cr,Tan}$ = load at first tangential crack; P_u = ultimate load; $P_{u,SC}$ = ultimate load of control slab; Δ_u = deflection corresponding the ultimate load, k = initial stiffness of a specimen ($k = P_{cr}/\Delta_{cr}$).

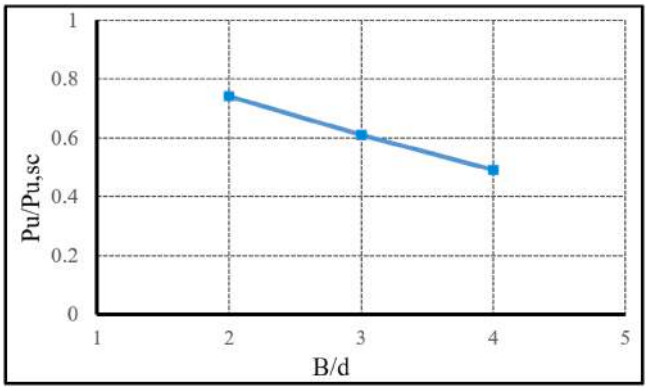


Fig. 6. Relation between ratio of $P_u/P_{u,sc}$ and B/d.

punching shear behaviour.

The location of the opening with respect to the supporting column is also a governing parameter on the punching shear strength of RC slabs. Fig. 7 presents a relation between the ultimate load/ultimate load of the control slab ($P_u/P_{u,sc}$) and the distance between the opening and column face/slab depth (X/d). As shown in Fig. 7, the capacities of the specimens with openings locating far from the column were larger than the capacity of the alternative slab with openings next to the column, however, the capacities of these slabs were still less than the control slab without opening. The capacity of slab S-SO-300-300 (with an opening 300 mm far from the column) was 36% higher than that of slab S-SO-300-0 (having an opening next to the column). However, the capacity of slab S-SO-300-300 was 18% less than that of the control slab without opening.

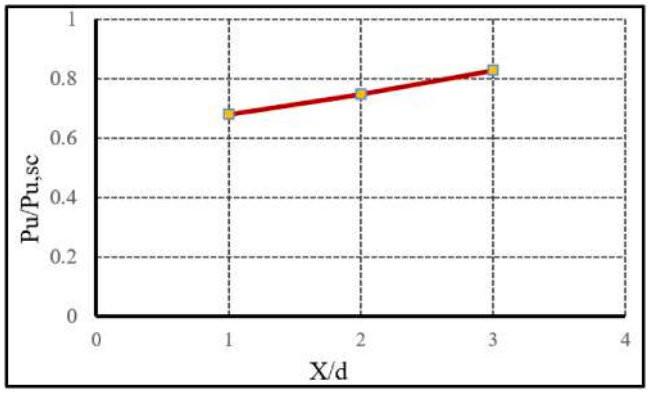


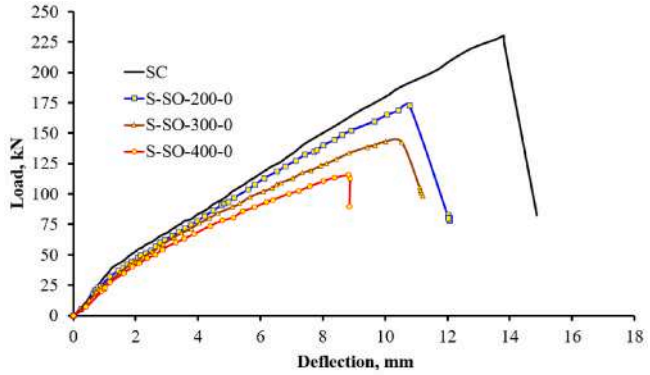
Fig. 7. Relation between ratio of $P_u/P_{u,sc}$ and X/d.

The specimens of group III were designed to study the effect of the opening shape. As shown in Table 5, the slabs with circular openings achieved ultimate loads higher than the slabs with square openings having similar openings areas. The punching shear capacities of slabs S-CO-250-0, S-CO-350-0 and S-CO-450-0 were 2.85, 18.88 and 30.43%, respectively, higher than those of slabs S-SO-200-0, S-SO-300-0 and S-SO-400-0.

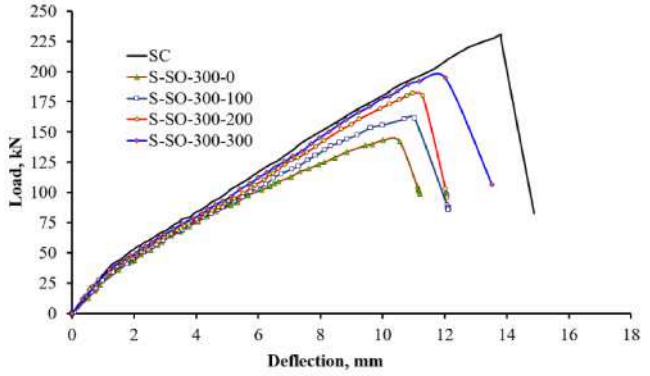
3.4. Load-deflection response

The load–deflection curves for the tested slabs are shown in Fig. 8. Table 5 presents the values of deflections at ultimate loads. In addition, Table 5 summarizes the values of the initial stiffness of the tested slabs. That was obtained by calculating the slope of the load–deflection curve in the un-cracked stage of loading [10]. As shown in Fig. 8, the tested slabs have a very similar trend throughout the loading stages. The load–deflection relationship was almost linear and the slabs have relatively similar stiffness up to the cracking load. A significant increase in the rate of the developed deflection could be observed after the formation of cracking. In addition, all slabs failed suddenly at the ultimate stage with an obvious drop in the load, which matches the manifested punching failure mode.

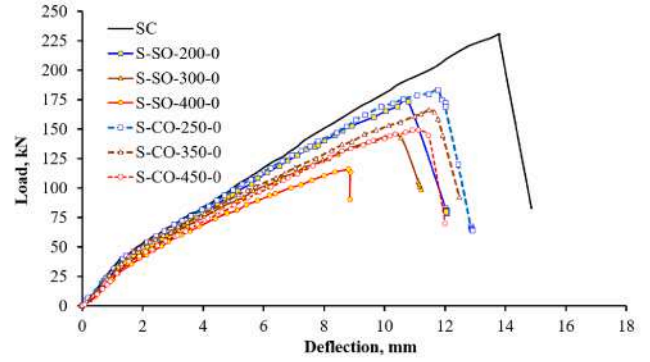
The load–deflection curves of group I are shown in Fig. 8a. Comparing the specimens of group I, it was found that, as the width of the opening increased, the stiffness of tested slabs decreased. That increased the measured deflection of the slabs with openings at all load levels. However, the deflection at ultimate decreased with the increase of the opening width. For slabs S-SO-200-0, S-SO-300-0 and S-SO-400-0, the values of deflections at ultimate were 10.84, 10.54 and 8.82 mm,



(a) Effect of opening dimensions



(b) Effect of opening location



(c) Effect of opening shape

Fig. 8. Load-deflection curves of the tested slabs.

respectively, these values represent 78, 76 and 64% of that achieved by the control slab ($\Delta_u = 13.81$ mm).

Group II was designed to study the effect of opening location on the punching shear behaviour of RC flat slabs. The load–deflection curves of group II are shown in Fig. 8b. As shown in Fig. 8b, the location of the opening did not affect the load–deflection response until approximately 50 kN (the occurrence of cracking). Beyond this level, whenever the opening was near the column (the zone of maximum stresses), the cracking stiffness of the slab decreased, thus the developed deflection increased. For instance, at a load of 100 kN, the deflection of slab S-SC-300-0 equals 6.1 mm vs 5.12 mm for slab S-SC-300-300.

The load–deflection curves of group III are shown in Fig. 8c. The slabs of group II are included in the figure for the purpose of comparison. As shown in Fig. 8c, the effect of the opening shape was clear with the increase in the opening size. As the slabs with circular openings had higher cracking stiffness than the slab with square openings. This may be attributed to the stress concentration at the sharp edges of the square

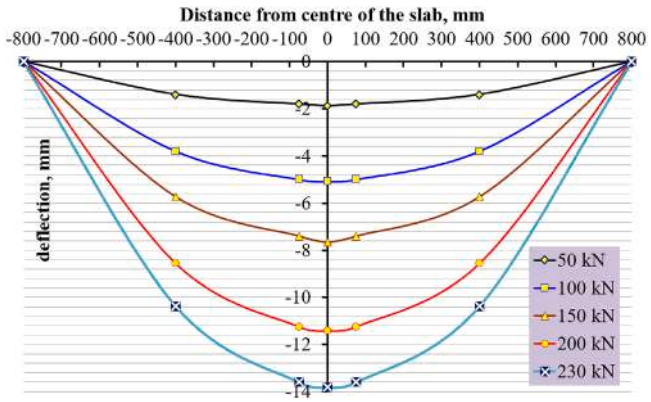
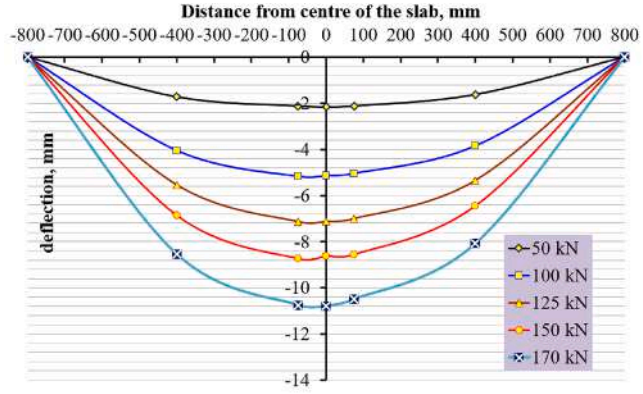
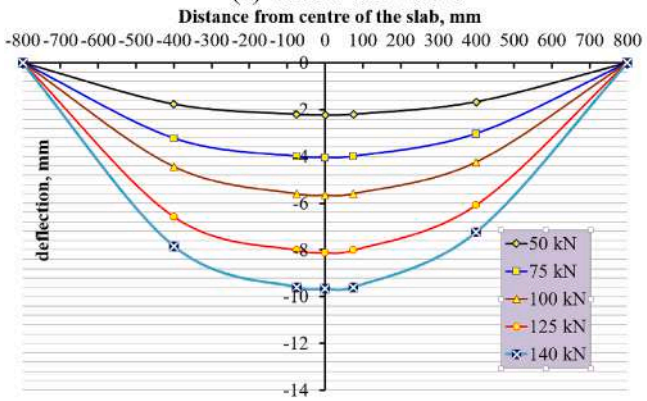


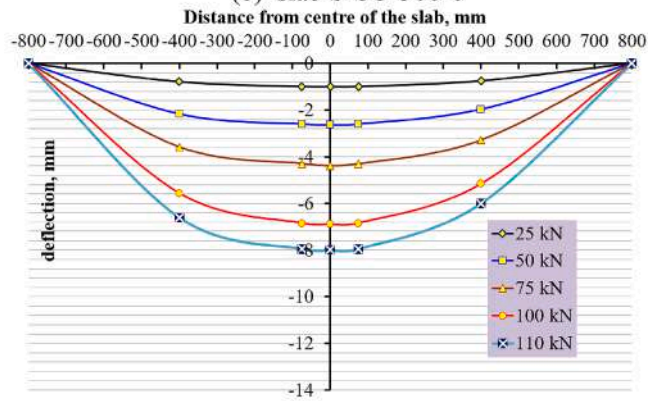
Fig. 9. Deflection profile of the control slab at different loads.



(a) slab S-SO-200-0



(b) slab S-SO-300-0



(c) slab S-SO-400-0

Fig. 10. Deflection profiles for group I at different loads.

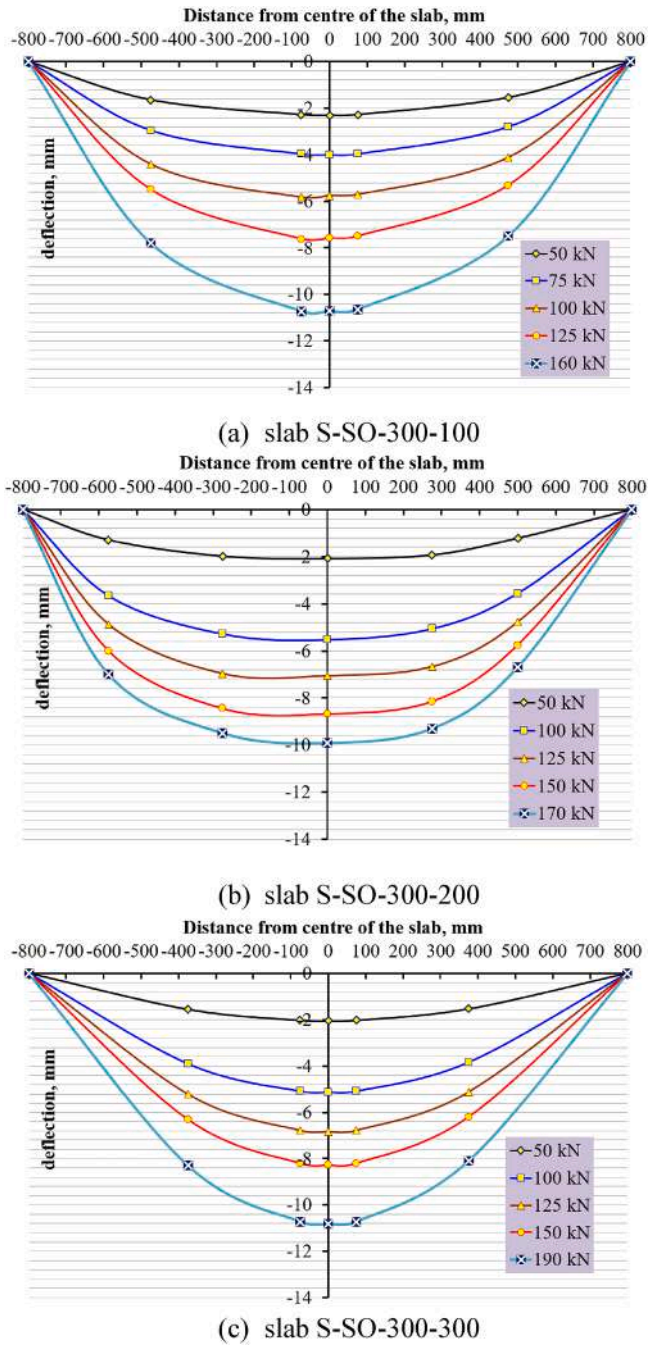


Fig. 11. Deflection profiles for group II at different loads.

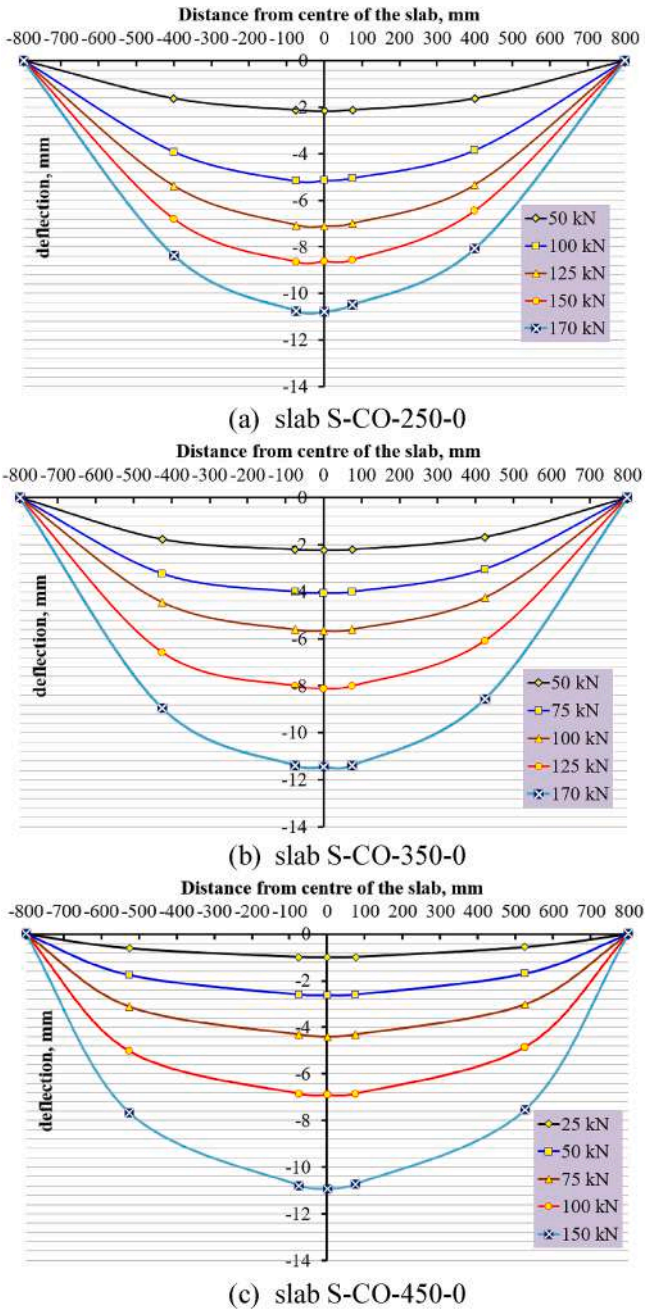


Fig. 12. Deflection profiles for group III at different loads.

opening, which led to a crack localization phenomenon at the opening's corners.

During the test, the displacements were measured at different locations along the centerline of the tested slabs to obtain the deflected profile. Figs. from 9–12 present the deflected profiles for all slabs. As can be seen in Fig. 9, the control slab (without opening) showed an almost asymmetrical profile for the vertical deflection in both sides of the stub column. As for the slabs with openings, the values of vertical deflections at the slab's left side (having an opening) were slightly higher than those of the slab's right side. The opening reduced the stiffness of the slabs and led to higher deflection at the area surrounding the opening).

3.5. Load-strain response

The load–strain curves of the main tension steel bars for the tested

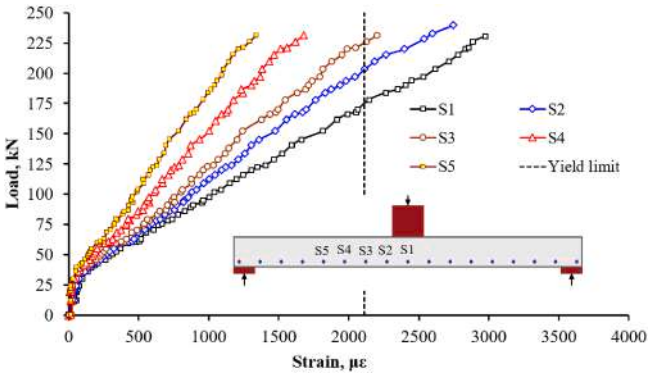


Fig. 13. Load strain curves of the control slab.

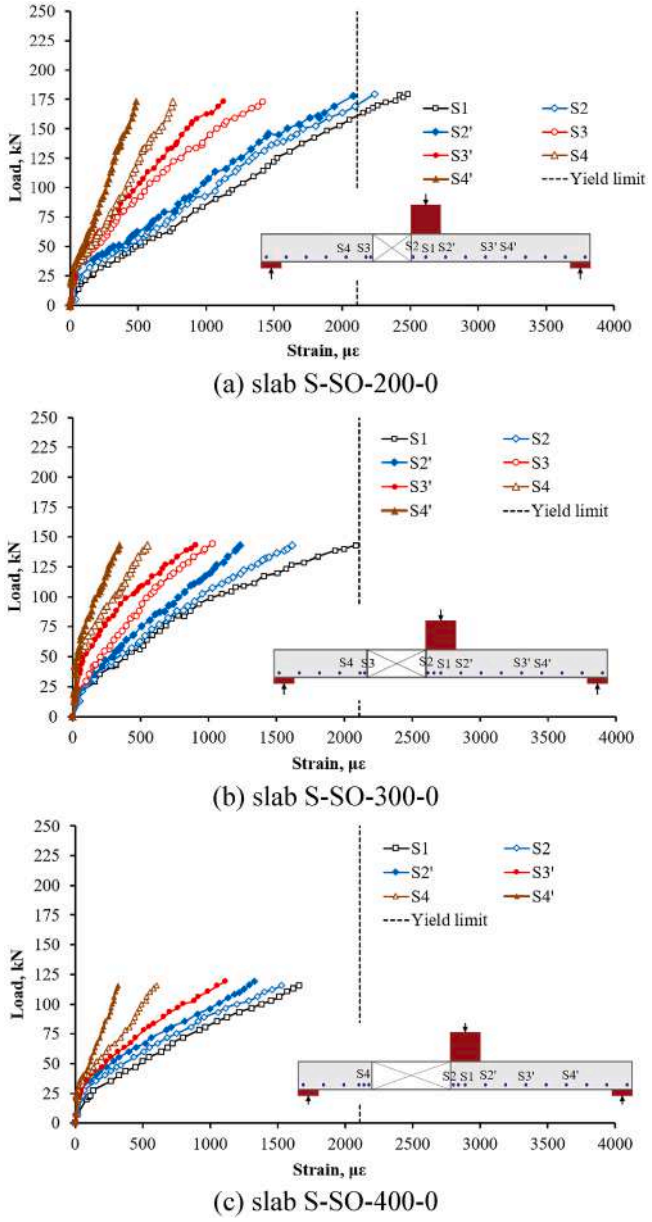


Fig. 14. Load strain curves of group I.

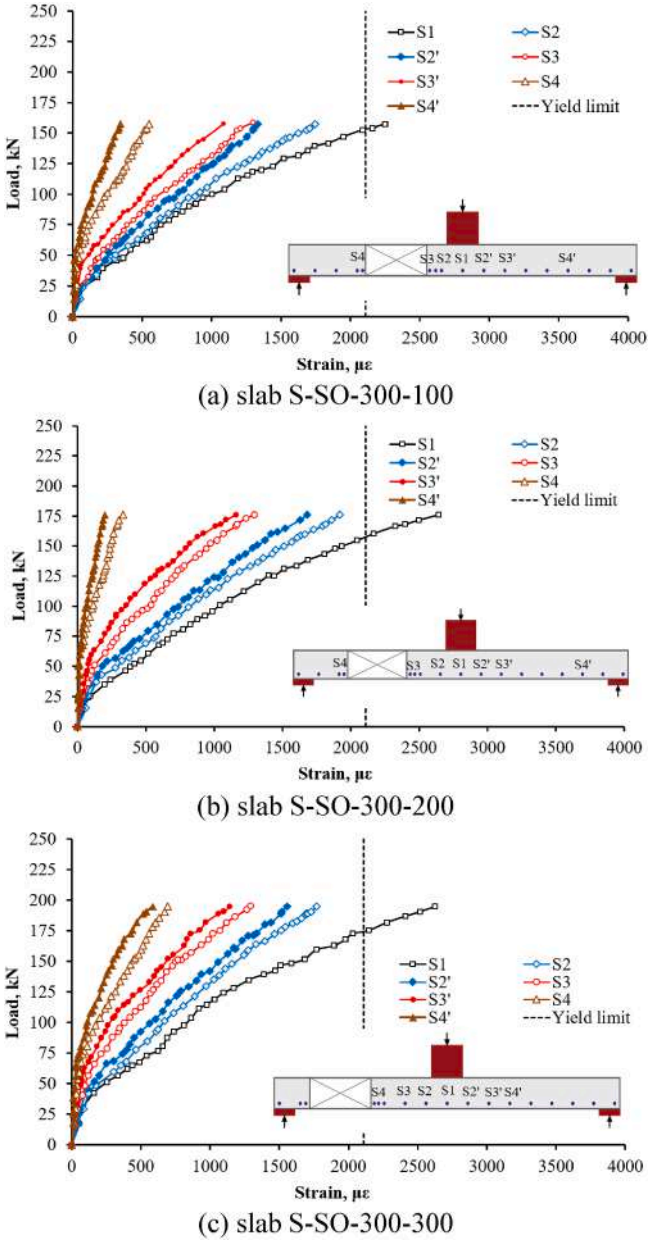


Fig. 15. Load strain curves of group II.

slabs are shown in Figs. from 13–16. Based on the steel reinforcement's mechanical characteristics, the yield strain was 2110 με. As shown in these figures, generally, the strain readings were insignificant till reaching the cracking of the concrete, beyond cracking, a significant increase in the rate of the developed strain was observed. As shown in the load–strain figures, most of the reinforcement bars did not reach the yield strain since the slabs exhibited punching shear failure mode. Moreover, as the opening size increased, the values of the ultimate strains decreased. For instance, at the middle reinforcement bar, the recorded strains at ultimate for slabs S-SO-200-00-0, S-SO-300-0 and S-SO-400-0, were 2480, 2082 and 1658 με, respectively. As the slabs with larger openings achieved lower failure loads. In addition, comparing the load strain curves of the same slab, it can be noticed that the strain values decreased as the bar was far from the column (I.e., the highest strains in the steel bars occurred in the bars near the middle of the slab). In addition, for a test slab with an opening, the bars at the side that included the opening recorded higher strains than their alternatives in the other side of the slab (without opening).

4. Prediction of punching shear strength in accordance with design code equations

In the current study, the ultimate punching shear capacities of the slabs were calculated using the equations of the available codes, ECP-203 [17], *ACI* 318-14 [18] and EC2 [19]. In the calculation of the punching capacity the mean values of material properties were used and the safety coefficients were not considered.

4.1. *ECP-203 code [17]*

As per the ECP-203 [17] code, the ultimate punching shear capacity (V_u) of slabs can be calculated as the smallest of the following equations:

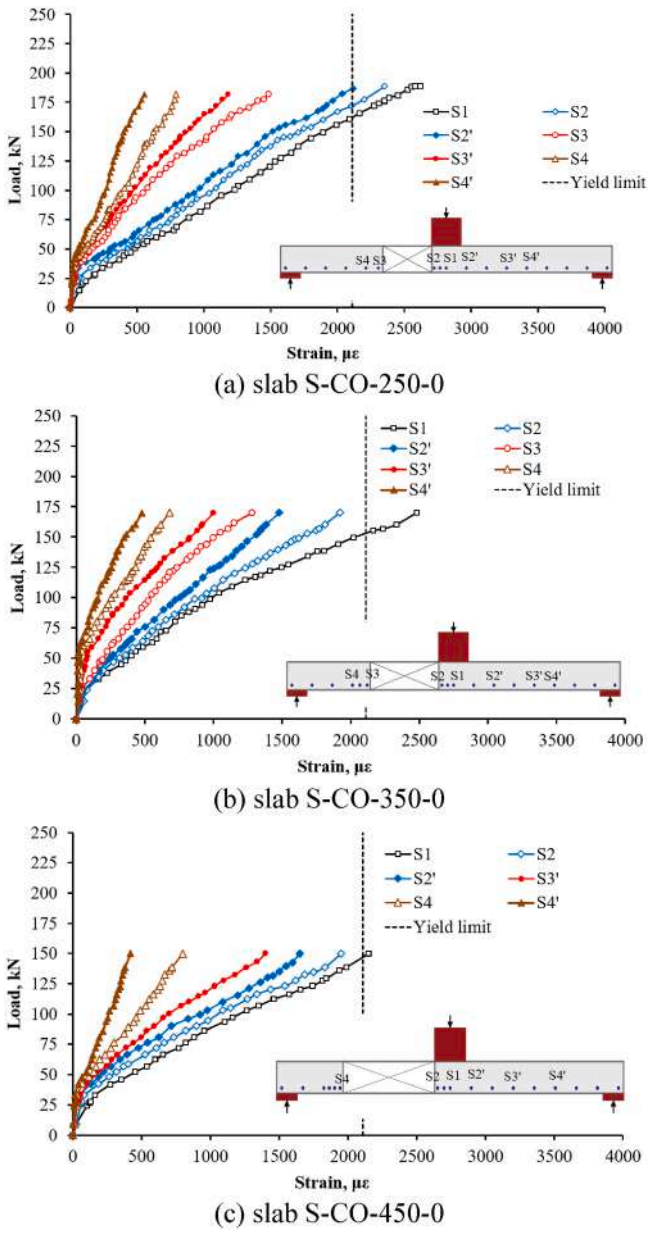


Fig. 16. Load strain curves of group III.

$$V_c \le \begin{cases} 0.8\left(\frac{\alpha.d}{b_o}+0.2\right)\sqrt{\frac{f_{cu}}{\gamma_c}}\,b_o d & (1) \\ 0.316\left(0.50+\frac{a}{b}\right)\sqrt{\frac{f_{cu}}{\gamma_c}}\,b_o d & (2) \\ 0.316\sqrt{\frac{f_{cu}}{\gamma_c}}\,b_o d & (3) \end{cases}$$

Where: b_o at d/2 from the column face.

4.2. ACI-318 code [18]

As per *ACI*-318 [18] code, the ultimate punching shear capacity (V_u) of slabs can be calculated as the smaller value of the following equations:

$$V_c \le \begin{cases} 0.17\left(1+\frac{2}{\beta}\right)\lambda\sqrt{f_c'}\,b_o d & (4) \\ 0.083\left(2+\frac{\alpha_s d}{b_0}\right)\lambda\sqrt{f_c'}\,b_o d & (5) \\ 0.33\lambda\sqrt{f_c'}\,b_o d & (6) \end{cases}$$

Where: b_o at d/2 from the column face.

4.3. EC2 code [19]

As per EC2 [19] code, the ultimate punching shear capacity (V_u) of slabs can be calculated using the following equations:

$$V_{Rd,c} = \left[C_{Rd,c}k(100\,\rho_1\,f_{ck})^{1/3} + k_1\sigma_{cp}\right]b_o d$$

$$k = 1+\sqrt{\frac{200}{d}} \le 2 \quad (8)$$

$$\rho_1 = \sqrt{\rho_{1x}\rho_{1y}} \le 0.02 \quad (9)$$

Where; b_o at 2d from the column face.

4.4. Comparison between the experimental results of the current research and codes' predictions

Table 6 presents a comparison between the experimental ultimate loads of the current research and the predicted loads of ECP-203, *ACI*-318 and EC2. As shown in Table 6, ECP-203 and *ACI*-318 showed conservative values for the ultimate loads for slabs with/without opening. The mean values of $V_{exp}/V_{pridected}$ were 1.38 and 1.20 for ECP-203 and *ACI*-318 codes, respectively. However, the safety margin of ECP-203 and

Table 6
Experimental ultimate loads versus codes' predictions.

Group	Slab's designation	P_{exp} kN	ECP-203 [17]		*ACI*-318 [18]		EC2 [19]	
			P_{ECP}, kN	$P_{exp}/P_{predicted}$	P_{ACI}, kN	$P_{exp}/P_{predicted}$	P_{EC2}, kN	$P_{exp}/P_{predicted}$
Control	SC	235	142	1.65	162	1.45	222	1.06
Group I	S-SO-200-0	175	113	1.55	129	1.36	169	1.04
	S-SO-300-0	143	92	1.55	110	1.30	154	0.92
	S-SO-400-0	115	84	1.37	96	1.20	146	0.78
Group II	S-SO-300-100	160	112	1.43	128	1.25	193	0.83
	S-SO-300-200	176	135	1.30	155	1.14	213	0.83
	S-SO-300-300	195	159	1.23	182	1.07	221	0.88
Group III	S-CO-250-0	180	141	1.28	162	1.11	246	0.73
	S-CO-350-0	170	135	1.26	155	1.10	229	0.74
	S-CO-450-0	150	130	1.15	148	1.01	218	0.69
Mean				1.38		1.20		0.85
Standard deviation				0.15		0.13		0.12
Coefficient of variation				0.11		0.11		0.14

P_{exp} = experimental ultimate load; $P_{predicted}$ = predicted ultimate load.

Table 7
Comparison of experimental test results of previous work and codes' predictions.

Ref.	Specimen	P_{exp}, kN	ECP-203 [17]		*ACI*-318 [18]		EC2 [19]	
			P_{ECP}, kN	$P_{exp}/P_{predicted}$	P_{ACI}, kN	$P_{exp}/P_{predicted}$	P_{EC2}, kN	$P_{exp}/P_{predicted}$
EL-Shafiey et al. [9]	1	427	297.01	1.43	280.22	1.52	253.09	1.68
	2	315	222.75	1.41	210.17	1.49	189.82	1.65
	3	222	198.00	1.12	186.81	1.18	173.37	1.28
	4	210	185.63	1.13	175.14	1.19	163.18	1.29
	5	339	247.50	1.37	233.52	1.45	214.73	1.58
	6	300	241.29	1.24	227.66	1.31	208.55	1.43
	7	261	237.60	1.09	224.18	1.16	204.8	1.27
Anil et al. [10]	1	193	158.02	1.22	180.71	1.07	180.06	1.07
	2	99.03	105.21	0.94	119.82	0.83	122.82	0.81
	3	125.86	129.10	0.98	165.74	0.76	148.23	0.85
	4	76.98	95.05	0.81	116.95	0.66	108.81	0.71
	5	94.70	125.52	0.76	160.75	0.59	140.95	0.67
	6	134.78	144.11	0.94	160.57	0.84	158.29	0.85
	7	172.15	139.25	1.24	160.13	1.08	162.42	1.06
	8	115.53	133.08	0.87	149.61	0.77	146.71	0.79
	9	138.83	135.26	1.02	150.71	0.92	153.72	0.90
Elsayed A. et al. [11]	1	97.5	61.21	1.59	70.32	1.39	116.30	0.84
	2	69.5	58.10	1.20	66.25	1.05	99.12	0.70
	3	88.5	54.30	1.64	62.42	1.42	101.25	0.88
	4	74.5	68.22	1.09	64.30	1.16	102.14	0.73
	5	81.3	57.25	1.43	65.45	1.25	105.09	0.77
	6	83.3	58.31	1.44	66.25	1.27	107.24	0.78
	7	88.5	59.24	1.50	67.20	1.32	108.21	0.82
Liberati et al. [12]	1	249.9	192.23	1.30	181.09	1.38	181.09	1.12
	2	216.4	189.82	1.14	178.84	1.21	178.84	0.98
	3	259.2	194.89	1.33	183.83	1.41	183.83	1.14
	4	232.3	191.98	1.21	180.08	1.29	180.08	1.04
	5	187.6	173.70	1.08	163.13	1.15	163.13	1.04
	6	178.0	167.92	1.06	157.52	1.13	157.52	1.01
	7	233.7	177.05	1.32	165.74	1.41	165.74	1.28
	8	187.6	133.05	1.41	125.07	1.50	125.07	1.37
	9	213.9	138.89	1.54	130.43	1.64	130.43	1.54
	10	194.8	133.42	1.46	126.49	1.54	126.49	1.43
	11	208.4	141.76	1.47	133.59	1.56	133.59	1.47
	12	184.0	138.34	1.33	130.50	1.41	130.49	1.38
Elsayed M. et al. [13]	1	182.9	93.4	1.96	106.9	1.71	141.2	1.29
	2	176.7	91.2	1.94	104.3	1.69	139	1.27
	3	154.9	87.6	1.77	100.2	1.55	135.3	1.14
	4	150.0	82.4	1.82	94.3	1.59	129.9	1.15
	5	140.2	70.1	2.00	80.1	1.75	105.9	1.32
	6	137.0	68.4	2.00	78.2	1.75	104.2	1.31
	7	119.2	65.7	1.82	75.2	1.59	101.5	1.18
	8	109.2	61.8	1.77	70.7	1.54	97.5	1.12
	9	120.4	62.3	1.93	71.2	1.69	94.2	1.28
	10	118.2	60.8	1.95	69.5	1.70	92.7	1.28
	11	100.9	58.4	1.73	66.8	1.51	90.3	1.12
	12	91.6	54.9	1.67	62.9	1.46	86.7	1.06
Summary of results including the results of the current research								
Mean				1.39		1.32		1.16
Standard deviation				0.31		0.27		0.26
Coefficient of variation				0.22		0.20		0.22

ACI-318 codes decreased with increasing the opening size or increasing the distance between the opening and the column. On the other hand, EC2 prediction model showed good results for the control slab and slab S-SO-200-0. The values of $V_{exp}/V_{pridected}$ were 1.06 and 1.04 for slab SC and S-SO-200-0, respectively. Whereas, for the remaining slab, EC2 code overestimated the ultimate capacity of the slabs with openings. The mean value of $V_{exp}/V_{pridected}$ was 0.85.

4.5. Comparison between the experimental results of previous research work and codes' predictions

Table 7 presents a comparison between the experimental results of previous work [9–13] for slabs with openings and those predicted by ECP-203, *ACI*-318 and EC2. The summary of the Table included the results of the current research. As shown in Table 7, the obtained results are consistent with those obtained by the current research. ECP-203 and *ACI*-318 showed higher factors of safety than EC2. The mean values of $V_{exp}/V_{pridected}$ for ECP-203, *ACI*-318 and EC2 codes were 1.39, 1.32 and 1.16, respectively.

5. Conclusion

Based on the carried-out experimental program on two-way RC slabs with/without openings the following conclusions can be drawn:

- Introducing an opening beside the column significantly reduced the punching shear capacity of the tested slabs. In addition, as the opening width increases, the reduction in the ultimate capacity increases. The reduction in the shear capacity reached about 51% with slab S-SO-400-0 with an opening width of 400 mm next to the column.
- The reduction in the ultimate capacity could be reduced by locating the opening far from the column and/or using a circular opening. The capacity of slab S-SO-300-300 (having an opening 300 mm far from the column) was 36% higher than that of slab S-SO-300-0 (having an opening next to the column). In addition, the punching shear capacity of slab S-CO-350-0 (having a circular opening with a diameter of 350 mm) was 18.88% higher than that of slab S-SO-300-0 (having a square opening with a size of 300 × 300 mm^2).
- The opening had a significant effect on the first cracking load. A great reduction in the cracking capacity of the slabs with openings was recorded. This reduction was increasing with increasing the opening size and decreasing with increasing the distance between the opening and the column. Also, the use of circular openings showed higher cracking loads compared to square openings.
- Comparing the load–deflection response of the tested slabs, the openings decreased the overall stiffness of the slabs with opening compared to the control slab, as well as, decreased the deflection at the ultimate load. Regarding the profile of deflection along the centerline of the slabs, the control slab showed an almost symmetrical deflection profile on both sides of the column. On the other hand, for the slabs with openings, the slab's side that includes an opening showed higher deflections than the other side.
- Based on the results of the current work, the prediction models of ECP-203 and *ACI*-318 showed conservative values for the ultimate loads for slabs with/without opening. The mean values of $V_{exp}/V_{pridected}$ were 1.38 and 1.20 for ECP-203 and *ACI*-318 codes, respectively. On the other hand, EC2 prediction model showed good results for the control slab and slab S-SO-200-0. Whereas, for the remaining slab, EC2 code overestimated the ultimate capacity of the slabs with openings. The mean value of $V_{exp}/V_{pridected}$ was 0.85.
- Based on the comparison between the results of a series of experimental works including the current research versus those predicted by ECP-203, *ACI*-318 and EC2 equations, ECP-203 and *ACI*-318 showed higher factors of safety than EC2. The mean values of $V_{exp}/V_{pridected}$ for ECP-203, *ACI*-318 and EC2 codes were 1.39, 1.32 and 1.16, respectively.

Declaration of Competing Interest

The authors declare that they have no known competing financial interests or personal relationships that could have appeared to influence the work reported in this paper.

References

[1] Yitzhaki D. Punching strength of reinforced concrete slabs. ACI 1996;63(5):527–61.
[2] Bu W, Polak MA. Effect of openings and shear bolt pattern in seismic retrofit of reinforced concrete slab–column connections. Eng Struct 2011;33:3329–40. https://doi.org/10.1016/j.engstruct.2011.05.025.
[3] Akhundzada H, Donchev T, Petkova D. Strengthening of slab-column connection against punching shear failure with CFRP laminates. Compos Struct 2019;208:656–64.
[4] Khalil A, Atta M, Hassan A, Abd-Elaaty A. Flexural strength recovery of RC one-way slabs having cut-outs using NSM-SHCC plates. Eng Struct 2022;258:114149. https://doi.org/10.1016/j.engstruct.2022.114149.
[5] Durucan C, Anil Ö. Effect of opening size and location on the punching shear behavior of interior slab-column connections strengthened with CFRP strips. Eng Struct 2015;105:22–36. https://doi.org/10.1016/j.engstruct.2015.09.033.
[6] Esfahani MR, Kianoush MR, Moradi AR. Punching shear strength of interior slab column connections strengthened with carbon fiber reinforced polymer sheets. Eng Struct 2009;31(7):1535–42.
[7] Esfahani MR. Effect of cyclic loading on punching shear strength of slabs strengthened with carbon fiber polymer sheets. Int J Civ Eng 2008;6(3):208–15.
[8] Meleka NN, Tayel MA, Ramadan AM. Strengthening RC slab-column connections with large openings using FRP woven wraps. Alexandria Eng J 2009;48(1):107–27.
[9] EL-Shafiey TF, Hussein M, Abdel-Aziz MA. (2011). Behaviour of flat slabs with openings adjacent to columns. International Conference of structural faults & repair 2012. At: Concrete Behaviour Part (CB) CB-AZIZ code. Volume: 2.
[10] Anil O, Kina T, Salmani V. Effect of opening size and location on punching shear behavior of two-way RC slabs. Mag Concr Res 2014. https://doi.org/10.1680/macr.14.00042.
[11] Elsayed A, Elsayed M, Saas DM. Punching shear behavior of RC flat plate with openings rested on coupled columns. International Journal of Advances in Mechanical and Civil Engineering, ISSN: 2394-2827, Volume-5, Issue-3, Jun.-2018.
[12] Liberatia EAP, Marquesa MG, Leoneld ED, Almeidaa LC, Trautweina LM. Failure analysis of punching in reinforced concrete flat slabs with openings adjacent to the column. Eng Struct 2019;182:331–43. https://doi.org/10.1016/j.engstruct.2018.11.073.
[13] Elsayed M, Tayeh BA, Kamal D. Effect of crumb rubber on the punching shear behaviour of reinforced concrete slabs with openings. Constr Build Mater 2021;311:125345.
[14] Genikomsou AS, Polak MA. Effect of openings on punching shear strength of reinforced concrete slabs-finite element investigation. ACI Struct J 2017;114:1249.
[15] Mostofinejad D, Jafarian N, Naderi A, Mostofinejad A, Salehi M. Effects of openings on the punching shear strength of reinforced concrete slabs. Structures 2020;25:760–73.
[16] Teng S, Cheong H, Kuang K, Geng J. Punching shear strength of slabs with openings and supported on rectangular columns. Struct J 2004;101(5):678–87.
[17] Egyptian code for design and construction of reinforced concrete structures (ECP 203-2020); 2020.
[18] ACI Committee 318 (2019). Building Code Requirements for Structural Concrete (ACI 318-19) and Commentary (ACI 318R-19). American Concrete Institute, Farmington Hills, MI, 519 pp.
[19] Eurocode No. 2. Design of concrete structures – part 1: general rules and rules for buildings. Commission of the European Communities, prEN 1992-1-1 draft; 2002.